

Time-Domain Passivity Control of Haptic Interfaces with Tunable Damping Hardware

Andrew H. C. Gosline and Vincent Hayward

Haptics Laboratory, Center For Intelligent Machines
McGill University, Montréal, Québec, H3A 2A7 Canada
E-mail: {andrewg, hayward}@cim.mcgill.ca

Abstract

We describe a time-domain passivity control methodology that uses programmable eddy current viscous dampers to prevent a user from extracting energy from a haptic interface. A passivity observer monitors the energy flow of the virtual environment, and damping hardware is used to remove any energy contributions from the virtual environment that violate passivity constraints. Experiments illustrate that the programmable physical damper method improves the performance of a haptic device that has minimal inherent dissipation.

1. Introduction

Haptic interface technology is a growing field of research in science and engineering. With haptic interfaces being sought in medical training, manufacturing, and perception research, the desire for high fidelity haptic interfaces increases steadily. The haptic interface hardware and control software each play a pivotal role in the fidelity of the interaction that a user can experience. Ideally, the hardware and software should be transparent so that the user can freely interact with the virtual environment [13]. However, it is difficult in practice to completely veil the complex electro-mechanical system with which the user is interacting. Cues come from a variety of sources including inertia, dry or viscous friction, and vibration.

Passivity theory states that a system is passive if the energy flowing in exceeds the energy flowing out. In haptics, creating a passive interface has been widely adopted. If the haptic interface is passive, the user cannot extract energy from it. Therefore, system passivity offers two major benefits: global stability, and the appearance of objects as passive in a virtual environment. By this reasoning, it is physically correct to enforce a passivity constraint on haptic interfaces.

In early work, Anderson and Spong performed passivity analysis for teleoperator systems with time delay [4]. Their system was divided into four passive subsystems, the human operator, master arm, slave arm, and the environment. Due to time delay, communication between the master and slave arm was nonpassive. Their work produced passive communication through active control. Similarly, Niemeyer and Slotine used passivity analysis and wave variable transforms to achieve stable teleoperation [19].

Passivity based analysis specific to haptic interface design and control has been studied by many researchers. Colgate and Schenkel used elegant theory to determine a passivity relationship between virtual stiffness, virtual damping, and physical damping for a sampled-data type haptic interface [8]. Their work clearly demonstrated that a passive haptic interface requires physical dissipation. Diolaiti *et al.* re-visited the theory to produce a more general result that includes contributions from quantization and coulomb friction [9]. Recently, Hulin *et al.* examined the stability contributions of physical damping in simulations and experiments with a haptic interface [14]. From these studies, passivity of a haptic system is clearly dependent on physical dissipation due to the existence of a non-zero time delay.

Rather than use passivity as an analytical tool only, Hanaford and Ryu proposed a time-domain passivity based control approach that was tested on the Excalibur haptic interface [12]. Their method employed two main components, a Passivity Observer (PO) and a Passivity Controller (PC). The PO monitors the system energy, and the PC modulates a virtual damping term to maintain a passivity constraint. It must be noted that the Excalibur display is cable driven, exhibiting considerable inherent dissipation [1], and that the authors indicated that their method was sensitive to a noisy velocity estimation signal. Recently, Ryu *et al.* applied a modified PO/PC scheme that used reference energy following to smooth the contributions of the PC and avoid exciting resonances in the PHANTOM haptic interface [20].

The benefits of tunable dissipative elements have been discussed in both hybrid [3, 17], and totally passive haptic

tic interfaces [7]. Passive interfaces have excellent stability characteristics, but are incapable of synthesizing a response in arbitrary directions. Much of the work with hybrid devices has used magnetorheological fluid (MR) or particle brakes, which are slow to actuate [10], and suffer from hysteresis [16]. In an alternate approach, the dissipative properties of a direct current (DC) motor have been investigated [18]. However, this method is not tunable, and the damping magnitude is limited to the back electromotive force (EMF) constant of the motor. In recent work, we demonstrated promising initial results with a hybrid haptic device that uses eddy current brakes (ECB) as tunable, linear, high bandwidth, viscous dampers [11].

Herein, we propose a time-domain passivity based control method that uses a PO to monitor the energy of the system, and a PC that actuates physical dampers to maintain system passivity. We also show that this method improves the stability of wall renderings.

2. Time-Domain Passivity

2.1. Theory and Definitions

Unlike an active system, a passive system cannot generate energy. In passivity control literature, sign convention states that energy dissipation is positive. Following [12], a one port system with effort, f , flow, v , and initial energy storage, $E(0)$, is passive if:

$$\int_0^t f(\tau)v(\tau)d\tau + E(0) \geq 0, \forall t \geq 0 \quad (1)$$

It follows that an M -port network is passive if:

$$\int_0^t [f_1(\tau)v_1(\tau) + \dots + f_M(\tau)v_M(\tau)]d\tau + E(0) \geq 0, \forall t \geq 0 \quad (2)$$

A Passivity Observer (PO) is a real-time numerical approximation of the energy flow in any portion of the interface and its control software. Assuming no initial energy storage, the PO is defined as:

$$E_{\text{obsv}}(n) = \Delta T \sum_{k=0}^n f(k)v(k) \quad (3)$$

where ΔT is the sampling period. The equivalent expression using joint variables is:

$$E_{\text{obsv}}(n) = \Delta T \sum_{k=0}^n \tau(k)\omega(k) \quad (4)$$

An impedance controlled haptic interface uses a serially connected PC to modulate the discrete force output based on

an input velocity. The first computation in the PC estimates a virtual damping coefficient that removes the active energy from the virtual environment using the update law:

$$\alpha(n) = \begin{cases} \frac{-E_{\text{obsv}}(n-1)}{\Delta T v(n)^2}, & \text{if } E_{\text{obsv}} < 0 \\ 0, & \text{if } E_{\text{obsv}} \geq 0 \end{cases} \quad (5)$$

where $\alpha(n)$ is the virtual damping force coefficient. Due to the introduction of this virtual damping coefficient, the PO update law is modified to account for energy removed by damping:

$$E_{\text{obsv}}(n) = E_{\text{obsv}}(n-1) + \Delta T f_{\text{VE}}(n)v(n) + \Delta T \alpha(n-1)v(n-1)^2 \quad (6)$$

The force output becomes:

$$f_{\text{output}}(n) = f_{\text{VE}}(n) + \alpha(n)v(n) \quad (7)$$

2.2. Limitations of Virtual Damping

The method described above maintains a passivity constraint by degrading system performance with additional virtual damping. As shown in Section 4.1, this technique is not well suited, for two reasons, to devices that have minimal inherent dissipation, such as a direct drive Pantograph. First, because the control signal is dependent on velocity estimation, we are forced to limit the virtual damping to avoid over-amplification of a noisy velocity signal. If a virtual damping coefficient of greater than approximately 3 Ns/m is used, vibration is generated that is audible and palpable despite the use of adaptive velocity estimation [15]. Second, at low velocity, when the effect of the added virtual damping is minimal, it is possible that insufficient physical dissipation could be unable to quench limit cycles near the boundary of a virtual wall.

3. Passivity Control with Tunable Dampers

While DC motors are passive elements, since they do not generate energy but convert it, obtaining programmable dissipation from them is difficult. Controlling the torque to oppose motion at all times can only be done to some approximation. In particular, time delay caused by sampling and reconstruction yields an erroneous signal each time the velocity changes sign. An additional confounding factor is that steady state velocity cannot be known better than a velocity quantum δ/T , where δ is the device resolution and T the time window allocated to estimate velocity. Methods that take advantage of known system dynamics and disturbance estimates to recover velocity from signals other than position alone are difficult to apply [5].

Rather than use actuators, such as motors, that were designed for purposes other than maintaining the passivity of a haptic interface, we propose to use eddy current brakes (ECB) that were specifically designed for this end. Since ECBs are passive by nature, and can be actuated at high frequency, they are ideally suited to remove prescribed quantities of energy without time delay and without dependence on a velocity estimation signal.

3.1. Hybrid Haptic Interface with Tunable Eddy Current Dampers

Fig. 1 shows the experimental device, as previously described in [11]. An ECB has been added to each base joint of the Pantograph haptic interface [6]. ECBs are simple magnetic devices that use the principle of eddy current induction. When a conductor moves in a magnetic field, closed loop currents are induced, and a resistive force is generated according to the Lorentz Force Law. ECBs are well suited for use as programmable dampers for haptic interfaces because they are fast to actuate, linearly viscous at low speeds [21], and do not add inherent dissipation.

The ECB blades are annular sections machined from electrical grade aluminum and fastened to each proximal arm such that they rotate concentrically around each motor axis. Aluminum is an ideal material for non-ferrous ECBs as it has low resistivity to maximize eddy current flow, and low density to minimize inertia. The toroidal electromagnets are constructed from a machined iron core wrapped with 24 gage enamel coated wire. This device is controlled at a fixed update rate of 10 kHz using a 2.0 GHz personal computer running Linux kernel 2.6 and the Xenomai real-time framework [22].

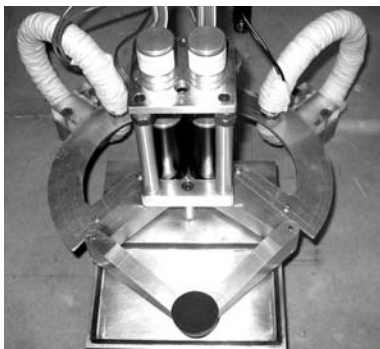


Figure 1. Hybrid pantograph with twin eddy current brakes.

The damping hardware has been upgraded from prior models with AMC 20A20 [2] PWM amplifiers that switch using a driving voltage of 200 V. This improvement results in a 1 ms rise time to 4 A of coil current, as shown in Fig. 2(a).

3.2. Passivity Control with Physical Dampers

According to [12], a prescribed amount of energy can be removed from a haptic interface with virtual damping by:

$$E_{diss} = \alpha v(n-1)^2 \Delta T \quad (8)$$

For the case of a pantograph with damped joints, it is more convenient to compute energy based on joint variables. Accordingly, Eq. (8) becomes:

$$E_{diss} = \beta \omega(n-1)^2 \Delta T \quad (9)$$

where ω is the angular velocity, and β is the damping torque coefficient of a joint.

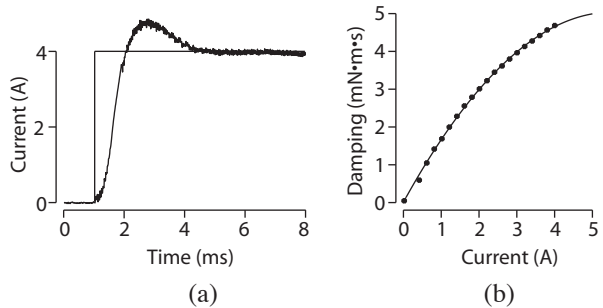


Figure 2. ECB Actuation Properties. (a) Step response to a 4 A current command. (b) Damping to coil current relationship.

The ECB dampers have a finite actuation time and a non-linear current to damping coefficient relationship (Fig. 2). Because the dampers require multiple update periods to actuate, their dynamics must be modeled and incorporated in the PC update. According to Fig. 2(a), the ECB amplifier and coil combination can be modeled with a linear slew rate of approximately 4000 A/s. Using a quadratic least squares fit, the damping coefficient to coil current plot in Fig. 2(b) was found to be:

$$\beta = -0.164 i_{coil}^2 + 1.81 i_{coil} \quad (10)$$

where i_{coil} is the coil current, making the update law for β :

$$\beta = -0.164(SR n_d \Delta T)^2 + 1.81(SR n_d \Delta T) \quad (11)$$

where n_d is the number of sampling periods expired since the dampers were activated and SR is the approximate slew rate of the amplifiers.

The control loop for the ECB damper PC, including the necessary saturation to protect the coils from overheating, is calculated by:

1. Update the PO:

$$E_{\text{obsv}}(n) = E_{\text{obsv}}(n-1) + \Delta T \tau_{\text{VE}}(n) \omega_{\text{VE}}(n) + \beta_a(n-1) \omega(n-1)^2 \Delta T \quad (12)$$

2. Compute the required damping: β_d

$$\beta_d(n) = \begin{cases} \frac{-E_{\text{obsv}}(n-1)}{\Delta T \omega(n)^2}, & \text{if } E_{\text{obsv}} < 0 \wedge \beta_d < \beta_{\text{max}} \\ \beta_{\text{max}}, & \text{if } E_{\text{obsv}} < 0 \wedge \beta_d > \beta_{\text{max}} \\ 0, & \text{if } E_{\text{obsv}} \geq 0 \end{cases} \quad (13)$$

3. Damper actuation logic:

- If $E_{\text{obsv}} < 0$ AND dampers off, set required current and begin counting n_d .
- If $E_{\text{obsv}} < 0$ AND dampers on, set required current and continue counting n_d .
- Else If $E_{\text{obsv}} > 0$, turn off dampers and reset $n_d = 0$

4. Update actual state of dampers, β_a , using Eq. (11) with $\Delta T = 0.1 \times 10^{-3}$ s, and SR = 4000 A/s:

$$\beta_a(n) = \begin{cases} 0.16 a n_d^2 + 0.4 b n_d, & \text{if } n_d \leq 10 \\ 16.0 a + 4.0 b, & \text{if } n_d > 10 \end{cases} \quad (14)$$

where $a = -0.164$ and $b = 1.81$ are the coefficients of the polynomial fit.

There are several limitations to the use of physical dampers for passivity control. First, as this method is dependent on additional hardware, a haptic interface would have to be equipped with programmable physical dampers to make use of this method. Second, as the dampers actuate slower than the motors, the system energy could be in the active region longer than if virtual damping was used.

4. Experimental Results

Experiments were performed to compare the performance of the conventional (virtually damped) PC and the physically damped PC. For these experiments, a virtual wall located at $x = 0$ was rendered with the Pantograph. Repeatable contact was simulated using a pre-tensioned elastic band to thrust and hold the manipulandum against the virtual wall. The elastic band allows us to closely examine the passivity characteristics of the device and control software without the fluctuating and dissipative properties of a human operator. Velocity estimation was computed using a previously described method with a window size of 16, and maximum number of outliers of 2 [15].

4.1. Conventional Passivity Controller

Fig. 3 shows results from experiments with the conventional PC. Figs. 3(a) and 3(b) show contact with a 1.5 N/mm linear spring wall, which is clearly active as the energy level becomes negative. Figs. 3(c) and 3(d) show contact with the same virtual wall, but using a conventional PC with a damping coefficient limit of 3 Ns/m. Fig. 3(d) shows the energy level for the conventional PC wall contact. Note that while the energy in Fig. 3(d) does not become negative, a limit cycle similar to that in Fig. 3(a) is present in Fig. 3(c), but at a reduced magnitude.

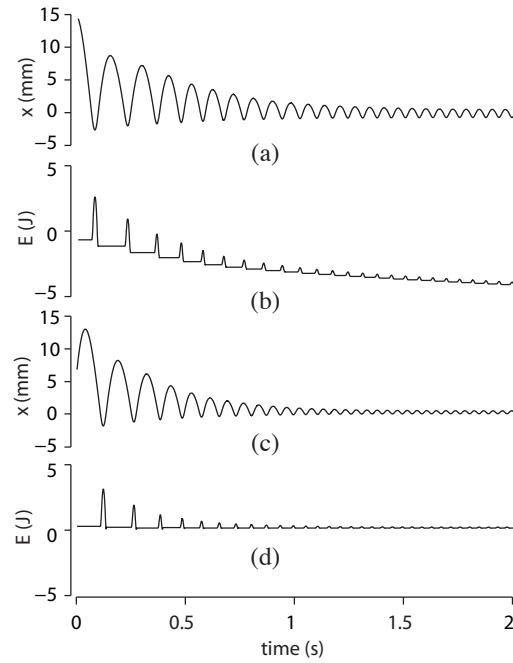


Figure 3. 1.5 N/mm virtual wall with conventional PC: (a) and (b) No PC, (c) and (d) PC with damping coefficient limit.

Fig. 4 shows results from wall contact when the physical dampers are used to create a very small amount of constant physical dissipation using a coil current of 0.4 A, corresponding to a damping torque coefficient of approximately 0.3 mNm/s in each joint. Though this amount of damping is practically imperceptible in free space, it has a noticeable impact on the wall contact results. Figs. 4(a) and 4(b) show wall contact without the conventional PC, while Figs. 4(c) and 4(d) show contact with the conventional PC. In both cases, the contribution of physical dissipation is evident. Compared to Fig. 3(a), the limit cycle shown in Fig. 4(a) is reduced in magnitude. Compared to Fig. 3(b), the energy level shown in Fig. 4(b) drops at a slower rate. The addition of a conventional PC also produces clear differences

when constant physical dissipation is added. Compared to Fig. 3(c), the limit cycle in Fig. 4(c) is eventually quenched. The energy level with a conventional PC, shown in Fig. 4(d), becomes stable and reaches zero. This experiment illustrates that the addition of a small amount of physical dissipation can stabilize the conventional PC rendering, which is in agreement with prior theoretical and experimental findings.

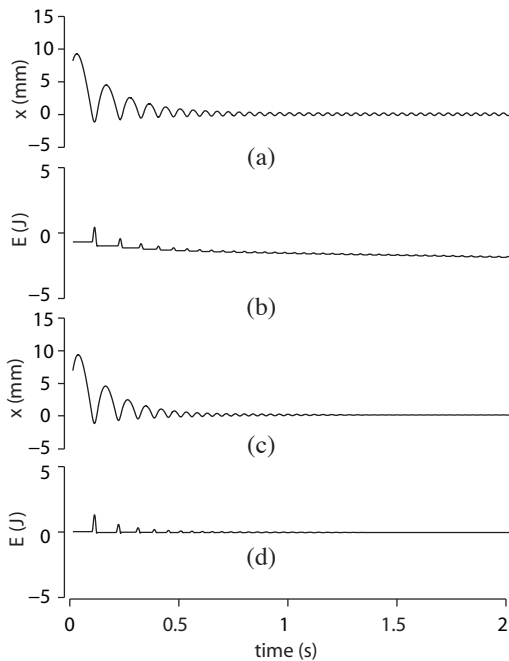


Figure 4. 1.5 N/mm virtual wall with conventional PC and constant physical damping: (a) and (b) No PC, (c) and (d) PC with damping coefficient limit.

Energy traces were computed using Eq. (3) for Figs. 3(b) and 4(b), and Eq. (6) for Figs. 3(d) and 4(d).

4.2. Physically Damped Passivity Controller

Fig. 5 shows results from experiments using the physically damped PC. It is important to notice that the physical damper PC can stabilize contact with the 1.5 N/mm wall, despite the large initial position. Variations in initial position throughout the experimental plots are due to hand release of the manipulandum from approximately the same initial displacement and user input of the data logging command. The important features of the plots are not the initial transient response, but rather the presence of a steady limit cycle after transients have diminished.

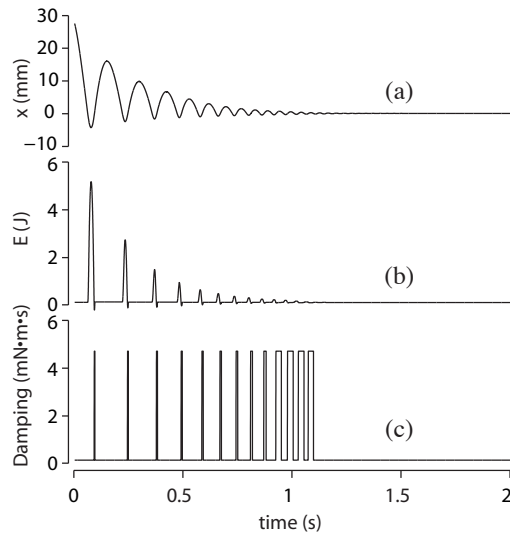


Figure 5. 1.5 N/mm virtual wall experiment with physical damping passivity controller.

Though not shown due to similarities and space constraints, the physically damped PC can also stabilize contact with a virtual wall at 3.0 N/mm. As in the 1.5 N/mm case, the conventional PC cannot stabilize the 3.0 N/mm virtual wall. At 3.0 N/mm, where the effects of motor saturation within the limit cycle are present, the results are very similar to those shown in Fig. 3 for the conventional PC and Fig. 5 for the physical PC. Only subtle differences are evident in 3.0 N/mm experiments. In the case of the conventional PC, the limit cycle has a slightly larger amplitude than is shown in Fig. 3(c). With the physical PC, the damping pulses are slightly longer than are shown in Fig. 5(c). The energy trace in Fig. 5(b) was computed using Eq. (12).

It is also interesting to note that the negative energy spikes shown in Fig. 3(d) on the trailing edge of the first four pulses are much smaller than the negative energy spikes in Fig. 5(b). This illustrates one limitation of using physical dampers that are slower to actuate than motors.

5. Conclusions and Future Work

An introduction to passivity based analysis in haptic interface control and a discussion regarding passive actuators for haptic interfaces were presented. A brief review of passivity theory was presented to familiarize the reader with the fundamentals of passivity control. A time-domain passivity control scheme that uses programmable physical dampers as dissipative elements has been developed and tested. Experiments illustrated the limitations of conventional passivity based control and the benefits of using programmable

physical dampers on a directly driven haptic interface with minimal inherent dissipation. Renderings that yield a steady limit cycle with conventional passivity control are stabilized when physical damping is substituted for its virtual counterpart.

Encouraging results indicate a number of potential improvements. First, as pointed out in [12], the PO requires resetting to prevent the time integral from unbounded growth, similar to classic integrator windup for PID control. For example, PO would amass a large quantity of dissipation due to friction when moving along a virtual wall with friction. If the integral was not reset prior to striking the wall again, the locally active wall contact would be seen as passive by the global PO. A multitude of potential cures for this problem are available, such as adaptive passivity window observation, or event based passivity observation. Each solution requires careful consideration and testing.

Finally, the benefits of using dissipative hardware in passivity control should also be investigated for teleoperation. As dissipative hardware does not suffer from the actuation problems associated with time delay, it could be used to provide high fidelity master arm control.

6. Acknowledgments

This work was funded by a Collaborative Research and Development Grant “High Fidelity Surgical Simulation” from the Natural Sciences and Engineering Council of Canada (NSERC), and by Immersion Corp., and by an NSERC-Discovery Grant. The authors would also like to acknowledge contributions and discussions from Gianni Campion, Jerome Pasquero, and Vincent Levesque.

References

- [1] R. Adams, M. Moreyra, and B. Hannaford. Excalibur, a Three-Axis Force Display. In *ASME Winter Annu. Meeting Haptics Symposium*, 1999.
- [2] Advanced Motion Controls. <http://www.a-m-c.com>. World Wide Web Page.
- [3] J. An and D. Kwon. Control of Multiple DOF Hybrid Haptic Interface with Active/Passive Actuators. In *Intelligent Robots and Systems, 2005. (IROS 2005)*, pages 2572–2577, 2005.
- [4] R. Anderson and M. Spong. Bilateral Control of Teleoperators with Time Delay. *IEEE Transactions on Robotics and Automation*, 34(5):494–501, 1989.
- [5] P. R. Bélanger. Estimation of Angular Velocity and Acceleration from Shaft Encoder Measurements. In *Proc. IEEE International Conference on Robotics and Automation*, pages 585–592, 1992.
- [6] G. Campion, Q. Wang, and V. Hayward. The Pantograph Mk-II: A Haptic Instrument. In *Proc. IROS 2005, IEEE/RSJ Int. Conf. Intelligent Robots and Systems*, pages 723–728, 2005.
- [7] C. Cho, M. Kim, and J. Song. Direct Control of a Passive Haptic Based on Passive Force Manipulability Ellipsoid Analysis. *International Journal of Control, Automation, and Systems*, 2(2):238–246, 2004.
- [8] J. E. Colgate and G. Schenkel. Passivity of a Class of Sampled-Data Systems: Application to Haptic Interfaces. In *Proc. of American Conference on Control*, pages 3236–3240, 1994.
- [9] N. Diolaiti, G. Niemeyer, F. Barbagli, and K. Salisbury. A Criterion for the Passivity of Haptic Devices. In *International Conference on Robotics and Automation*, pages 2463–2468, 2005.
- [10] M. Gogola and M. Goldfarb. Design of a PZT-Actuated Proportional Drum Brake. *IEEE Transactions on Mechatronics*, 4(4):409–416, 1999.
- [11] A. Gosline, G. Campion, and V. Hayward. On the use of Eddy Current Brakes as Tunable, Fast Turn-on Viscous Dampers for Haptic Rendering. In *Proceedings of Euro-Haptics*, pages 229–234, 2006.
- [12] B. Hannaford and J. Ryu. Time-Domain Passivity Control of Haptic Interfaces. *IEEE Transactions on Robotics and Automation*, 18(1):1–10, 2002.
- [13] V. Hayward and O. Astley. Performance Measures For Haptic Interfaces. In *In Robotics Research: The 7th International Symposium*, pages 195–207, 1996.
- [14] T. Hulin, C. Preusche, and G. Hirzinger. Stability Boundary for Haptic Rendering: Influence of Physical Damping. In *Proceedings of IROS*, 2006.
- [15] F. Janabi-Sharifi, V. Hayward, and C.-S. J. Chen. Discrete-Time Adaptive Windowing For Velocity Estimation. *IEEE Transactions on Control Systems Technology*, 8(6):1003–1009, 2000.
- [16] C. L. Kapuscinski. Motor Selection and Damper Design for a Six Degree of Freedom Haptic Display. Master’s thesis, Northwestern University, 1997.
- [17] T. B. Kwon and J. Song. Force Display using a Hybrid Haptic Device Composed of Motors and Brakes. *Mechatronics*, 16:249–257, 2006.
- [18] J. S. Mehling, J. E. Colgate, and M. A. Peshkin. Increasing the Impedance Range of a Haptic Display by adding Electrical Damping. In *Proc. of the First Joint Eurohaptics Conference and Symposium on Haptic Interfaces for Virtual Environment and Teleoperator Systems WHC’05*, pages 257 – 262, 2005.
- [19] G. Niemeyer and J. J. Slotine. Stable Adaptive Teleoperation. *IEEE Journal of Oceanic Engineering*, 16(1):152–162, 1991.
- [20] J. Ryu, C. Preusche, B. Hannaford, and G. Hirzinger. Time Domain Passivity Control With Reference Energy Following. *IEEE Transactions on Control Systems Technology*, 13(5):737–742, 2005.
- [21] H. D. Wiederick, H. Gauthier, D. A. Campbell, and P. Rochon. Magnetic Braking: Simple Theory and Experiment. *American Journal of Physics*, 55(6):500–503, 1987.
- [22] Xenomai Real-time Framework for Linux. <http://www.xenomai.org>. World Wide Web Page.